J Mater Sci (2006) 41:7524–7529
DOI 10.1007/s10853-006-0836-7

Effects of microalloying and ceramic particulates on mechanical properties of TiAl-based alloys

L. M. Peng · Z. Li · H. Li

Received: 26 September 2005 / Accepted: 9 November 2005 / Published online: 19 September 2006

Abstract Micro-alloyed titanium aluminides and TiAl-based composite with a fully dense structure have been synthesized by a powder metallurgical method. X-ray diffraction and EDX studies show that the monolithic TiAl-based alloy and its composite consist of TiAl and Ti_3Al compounds with the former as the major phase. Additions of Nb and/or (Mo + Cr) exert remarkable effects on the resultant phase compositions and mechanical properties of TiAl-based alloys. Both the added Mo and Cr elements are dissolved into the TiAl-based compounds to exhibit solid solution strengthening effect whereas Nb is only partially dissolved and the rest appears in the Nb-rich compound, Nb_2Al. In general, the micro-alloyed TiAl and the composite exhibit superior flexural strength and fracture toughness to TiAl-based monolithic compound.

Introduction

During the last two decades, TiAl-based alloys with compositions slightly on the titanium-rich side of stoichiometry, yielding two-phase structures of γ-TiAl (major) and α_2-Ti_3Al (minor) have been intensively studied. They are being recognized as substitutes for conventional nickel-based superalloys as weight-saving structural materials in some gas turbine engineering applications due to some attractive properties such as low density, high specific strength, high specific stiffness, high temperature strength retention, and good environmental resistance [1–4]. Unfortunately, despite the achievement of significant improvements in the mechanical properties and corrosion resistance of titanium aluminide alloys, the widespread use of these alloys has been limited by a relatively poor balance of room-temperature strength/ductility and fracture/creep resistance, and uncertain feasibility of economic fabrication technical routes.

Accordingly, continued attempts have been made with the purpose of enhancing the room temperature fracture toughness while maintaining the superior oxidation resistance as well as acceptable strength of TiAl-based alloys at elevated temperatures. One of the routes to overcome the above-mentioned deficiencies is alloying additions. To date, various TiAl-based alloys have been developed [1, 5, 6]. For instance, engineering gamma TiAl alloys were recently designed with a broad composition range of (in at.%) of Ti-(44–48) Al-(0–2)(Cr, Mn)-(0–10)Nb-(0–1)(W, Hf, Mo, Zr)-(0–1)B-(0–0.2)C-(0–0.3)Si, with intention to enhance ductility (Nb, Cr), strength (Mo), oxidation (Nb, W) and creep (C, Si and Mo) resistance through solid solution and/or precipitation hardening effect [7, 8]. In particular, it is well established that Nb can improve the room temperature ductility of the brittle ordered intermetallic α_2 (Ti_3Al) phase. Moreover, increases in Nb are usually associated with decrease in Al content, which results in enhanced strength levels [9–11]. Another

L. M. Peng (✉) · Z. Li
CAS Key Laboratory of Mechanical Behavior and Design of Materials, School of Engineering Science, University of Science and Technology of China, Hefei 230026, Anhui, P.R. China
e-mail: penglm@ustc.edu.cn

H. Li
Research Institute of Micro/Nano Science and Technology, Shanghai Jiaotong University, Shanghai 200030, P.R. China

Table 1 Chemical composition of raw powder mixtures

Powder mixture	Composition (wt.%)						
	Ti	Al	Nb	Mo	Cr	Al_2O_3	TiC
Ti–Al	64	36	–	–	–	–	–
Ti–Al–Nb	59	33	8	–	–	–	–
Ti–Al–Nb–Mo–Cr	59	33	5	2	1	–	–
Ti–Al–Al_2O_3–TiC	51	29	–	–	–	5	15

effective approach is adding reinforcements to obtain multiphase microstructures or TiAl-based composites [12–15].

The present study is aimed at the investigation of Nb combined with additions of Cr and Mo on the mechanical properties of TiAl-based alloys fabricated through the powder metallurgical technique. Monolithic compound based on Ti–Al and its composite reinforced with *external combinative addition* of micro-sized Al_2O_3 and TiC are also prepared using the same processing route for a comparison purpose. The resultant phases in the products, their microstructure and mechanical properties are examined.

Experimental description

As presented in Table 1, four powder mixtures are prepared from high purity raw fine powders (~325 mesh in size) of 99.99%Ti, 99.99Al%, 99.5%Nb, 99.99%Mo, 99.99%Cr, 99.9% α-Al_2O_3 (1 μm) and 99.9%TiC (1 ~ 3 μm) in purity by wet ball-milling in ethanol for 24 h. The ratio of Ti and Al atoms in the four powder blends is constant at approximately 1/1. The slurries are dried at 80 °C for 10 h in vacuum, and then uniaxially die-pressed under 300 MPa into platelets. Sintering is performed in vacuum, by uniaxial hot-pressing under 20 MPa at 1100 °C for 2 h in a BN-coated graphite die. Pressure is applied at 650 °C during the heating and released at the same temperature during cooling.

Rectangular bars for the bending tests are cut to the final dimensions of $3 \times 4 \times 40$ mm^3 by means of electro-discharge machining (EDM) from the sintered samples. Single edge notched bend (SENB) specimens with *a/W* (where *a* = notch depth) = 0.5 are fabricated following the ASTM E-399 specifications [16]. The specimens are ground and polished using standard

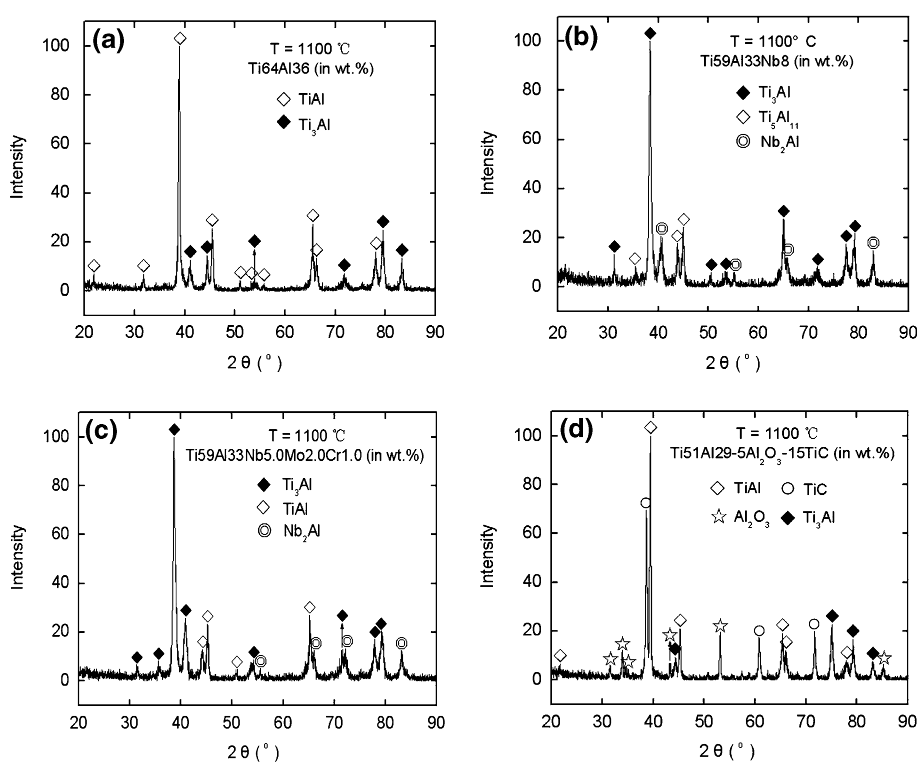

Fig. 1 XRD patterns for samples (**a**) TiAl, (**b**) TiAl–Nb, (**c**) TiAl–Nb–Mo–Cr and (**d**) TiAl–Al_2O_3–TiC composite after hot-pressed sintering under 20 MPa at 1100 °C for 2 h

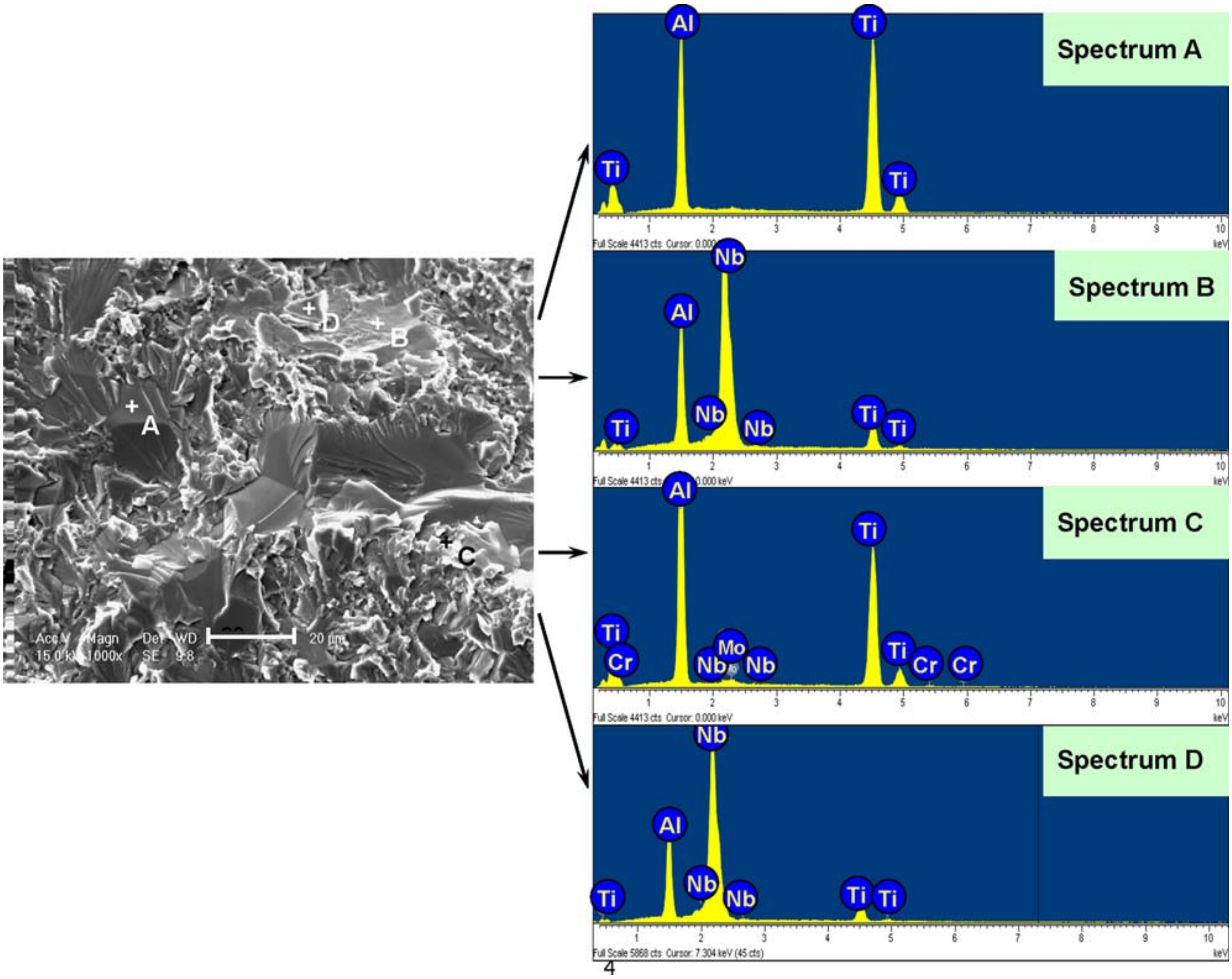

Fig. 2 EDX spectra for TiAl–Nb–Mo–Cr alloy to indicate the trace of alloy elements in the intermetallic compounds

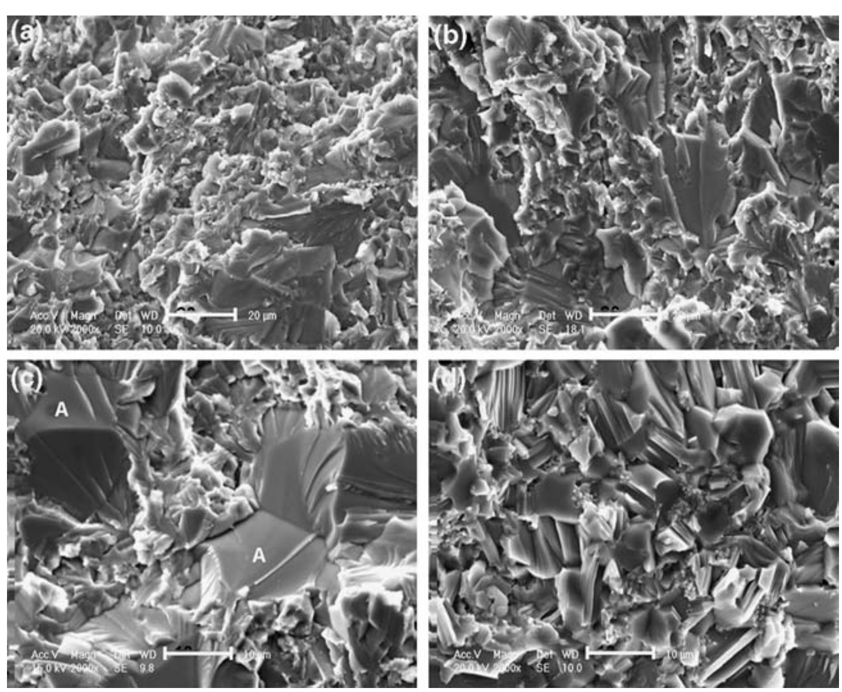

Fig. 3 Scanning electron microscopy (SEM) imagines of (**a**) TiAl, (**b**) TiAl–Nb, (**c**) TiAl–Nb–Mo–Cr alloys and (**d**) TiAl–Al_2O_3–TiC composite

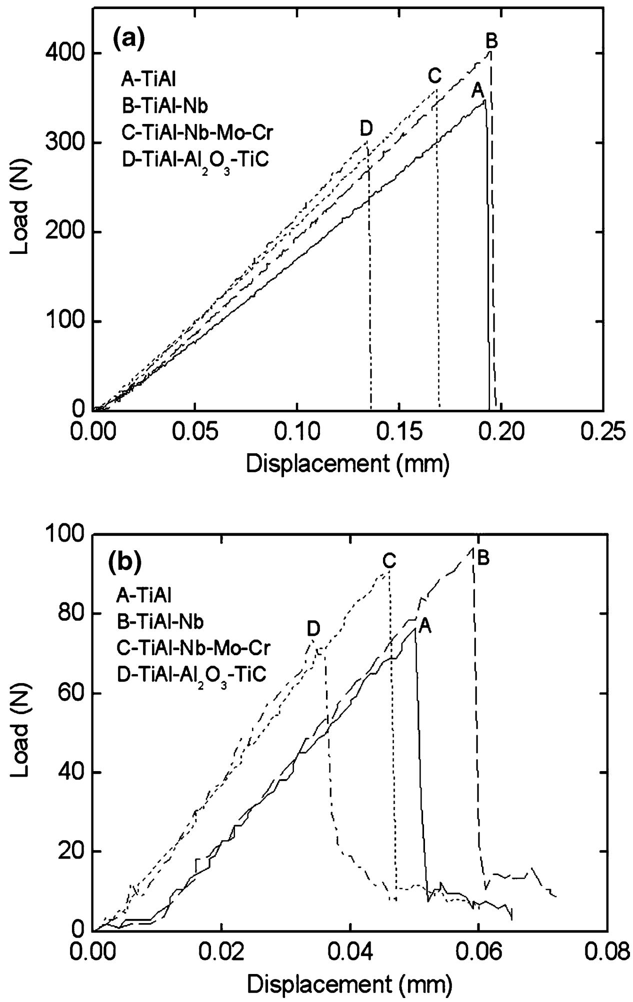

Fig. 4 Typical load–displacement curves of the synthesized materials at room temperature from (**a**) four-point bending and (**b**) fracture toughness tests

metallographic techniques. Both the flexural strength and fracture toughness measurements are carried out through a three-point bending test with a loading span of 30 mm and a cross-head speed of 0.5 mm/min on a Shimadzu machine. The variations between load and displacement are automatically recorded by the computer connected with the machine. At least five specimens are measured for each material. The resultant phases in the sintered compacts are identified by X-ray diffraction (XRD) with Cu-$K\alpha$ radiation at 40 kV and 40 mA. The microstructures of the fracture surfaces after mechanical tests are observed using a PHILIPS XL-30 SEM.

Table 2 Room temperature mechanical properties of TiAl-based compound and its composites

Materials	Flexural strength, σ_f (MPa)	Fracture toughness, K_{IC} (Mpa $\sqrt{m}$)
Ti–Al	360	3.8
Ti–Al–Nb	472	8.0
Ti–Al–Nb–Mo–Cr	446	7.8
Ti–Al–Al_2O_3–TiC	407	6.4

Results and discussion

The XRD patterns of the four powder mixtures after hot-pressed reactively sintered are shown in Fig. 1. It is evident that all the materials appear to have undergone complete reaction and multiphases are obtained since no unreacted elemental components are detected The Ti50–Al50 material and TiAl-based composite reinforced with Al_2O_3 and TiC particulates contain both types of TiAl and Ti_3Al with the former as the major compound. However, although the other two compacts containing Nb and/or (Mo + Cr) have stoichiometric Ti/Al atomic ratios, Ti_3Al accounts for the major phase since a part of Al is consumed through the reaction with Nb in the former two mixtures. Additionally, it should be noted that small amounts of Al will be lost through vaporization during the hot-pressing process. Previous study has demonstrated that by mechanical alloying of Ti–Al powder blends with different Al compositions, as well as by dry ball milling of Ti–aluminides for long milling times, h.c.p metastable solid solutions were formed for Al concentrations up to 60 at.% and an f.c.c. metastable solid solution for 75 at.% due to chemical disordering [17]. Nevertheless, in the present study, the powder blends are wet ball milled and the reactions among the elemental powders occur during the subsequent sintering process instead of during the ball milling process. Moreover, the formation of TiAl-based compounds is consistent with the phase relationship in the Ti–Al binary phase diagram. As evident from the EDX spectra in Fig. 2 for TiAl–Nb–Mo–Cr alloy, both the added Mo and Cr elements are dissolved into the TiAl-based compounds.

It has shown that Nb is completely solved without the formation of any Nb-bearing compounds in Ti–Al–Nb alloys fabricated by ingot metallurgy [8, 18–20]. However, the present investigation has indicated that Nb is only partially dissolved and the rest appears in the Nb-rich compound, Nb_2Al as indicated in the XRD patterns (Fig. 1b, c). The relevant XRD data for this phase as identified in Fig. 1b, i.e. the space distances, d as 0.22255, 0.16637, 0.14200 and 0.11636 nm at corresponding peaks of 40.5, 55.2, 65.7 and 82.9°, are in good agreement with those taken from the PDF card (No. 140458) where d takes corresponding values of 0.22220, 0.16590, 0.14200 and 0.11600 nm. Oehring et al's study

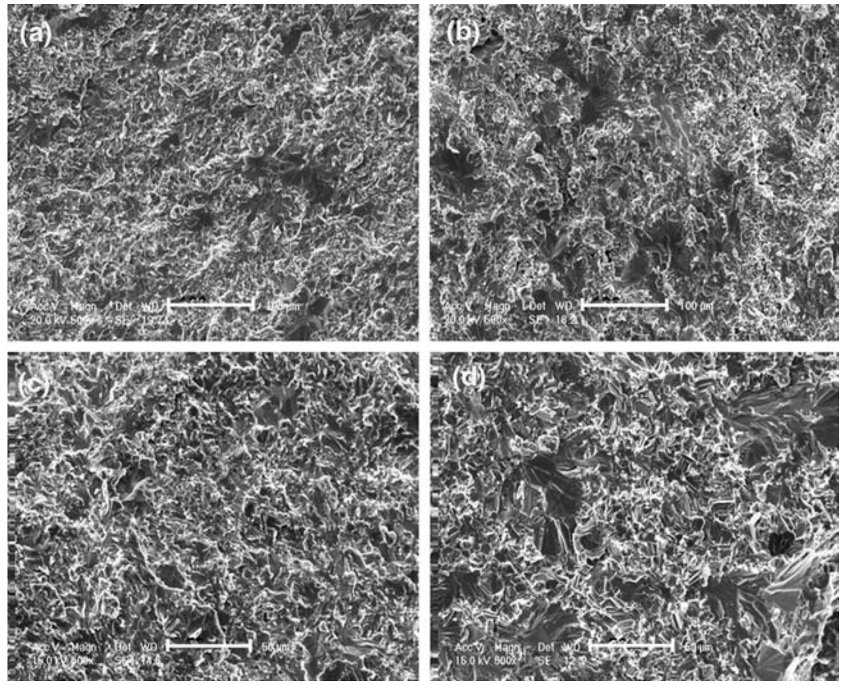

Fig. 5 Fracture surfaces of (**a**) TiAl, (**b**) TiAl–Nb, (**c**) TiAl–Nb–Mo–Cr and (**d**) TiAl–Al_2O_3–TiC composite after bending test at room temperature

[21] has shown that the A15 phase, Nb_3Al in the Nb-25 at.% Al system can almost completely be transformed into a supersaturated bcc NbAl solid solution, whereas the Nb_2Al phase is more stable in agreement with its higher thermodynamical stability with respect to the bcc phase and still exists even after long term dry ball milling. The results obtained by Buta et al. also indicate that Nb_2Al phase is more stable than Nb_3Al and can be formed within a composition range of 30 ~ 42 at.% Al, as shown tin the Nb–Al binary phase diagram [22, 23]. In the present study, since most of Al reacts with Ti to form Ti–Al compounds and only small part with Nb, yielding Nb_2Al phase.

Figure 3a through d show the microstructures of the four sintered compacts after hot-pressed reactive sintering at 1100 °C for 2 h. It can be found that all the materials are fully dense. In case of TiAl–Nb–Mo–Cr alloy, there exist some large colonies of Ti_3Al as marked by A in Fig. 3c. On the other hand, the composite is characterized by a lamellar structure, which may be attributed to the grain growth restricting effect exerted by the small Al_2O_3 and TiC particles in certain crystallographic orientations. These particles tend to agglomerate and are situated at colony boundaries (Fig. 3d).

As indicated from the typical load–displacement curves in Fig. 4, all materials fail with the sudden drop in load at the peak value during testing since they possess linear load–displacement curves, revealing an unstable crack propagation. Table 2 lists the room temperature flexural strength and fracture toughness properties of the four materials. The average value of flexural strength is 360, 472, 446 and 407 MPa for monolithic Ti50–Al50, TiAl–Nb, TiAl–Nb–Mo–Cr alloys and TiAl–Al_2O_3–TiC composites, respectively. The related fracture toughness is 3.8, 8.0, 7.8 and 6.4 MPa $\sqrt{m}$, respectively. It can be found that the Nb containing TiAl-based alloy has the highest values of both flexural strength and fracture toughness. In particular, it exhibits fracture toughness two times that of the monolithic TiAl-based alloy. In case of TiAl–Nb–Mo–Cr alloy, where a part of Nb is replaced by Mo and Cr, both the strength and fracture toughness decrease slightly. However, the micro-alloyed TiAl and the composite exhibit superior mechanical properties to TiAl-based monolithic compound. It is well documented that single γ-TiAl phase suffers from poor ductility and fracture toughness at ambient temperature [1]. For stoichiometric TiAl alloy, significant shifts of phase composition may take place in case Nb is added (Fig. 1a through c). It has been found by Chen et al. that Nb addition increases the eutectoid temperature of the Ti–Al system, and decreases the Ti_3Al (α) transus and the minimum Al solubility in TiAl (γ) phase [24]. Under such a circumstance, the β-phase field is extended by Nb addition to higher Al concentration, but contracts the α-phase field. As a result, the γ-TiAl phase field in the Ti–Al–Nb is inclined to the Ti side, which will decrease Al content and increase Ti + Nb contents in the γ-TiAl phase. In this case, solution hardening and precipitation strengthening occurs. For the composite, the toughening effect might arise from interaction between the crack tip and the fine ceramic particles [15]. Figure 5 shows the fracture surfaces of the four materials. In general, all of them exhibit a typical transgranular cleavage fracture mode.

Summary

Three TiAl alloys and TiAl-based composite reinforced with fine ceramic particulates are fabricated using a power metallurgical method (hot-pressed sintering). There microstructures and mechanical properties are evaluated. The results show that the properties of TiAl-based alloys can be significantly altered by Nb and/or (Mo + Cr) additions and ceramic particles. In particular, the micro-alloying of Nb apparently results in the highest mechanical properties among the four materials.

Acknowledgements The financial supports to LMP by SRF for ROCS, SEM and USTC are gratefully acknowledged.

References

1. Appel F, Wagner R (1998) Mater Sci Eng R22:187
2. Yamaguchi M, Inui H, Ito K (2000) Acta Mater 48:307
3. Li ZX, Cao CC (2005) Intermetallics 13:251
4. Saari H, Beddoes J, Seo DY, Zhao L (2005) Intermetallics 13:937
5. Hu D, Godfrey AB, Blenkinsop PA, Loretto MH (1998) Metall Mater Trans 29A:919
6. Cheng TT, Loretto MH (1998) Acta Mater 46:4801
7. Kim Y-W, Dimiduk DM (1991) JOM 43:40
8. Carneiro T, Kim Y-W (2005) Intermetallics 13:1000
9. Paul JDH, Appel F, Wagner R (1998) Acta Mater 46:1075
10. Zhang WJ, Deevi SC, Chen GL (2002) Intermetallics 10:403
11. Germann L, Banerjee D, Guedou JY, Strdel J-L (2005) Intermetallics 13:920
12. Soboyejo WO, Venkateswararao KT, Satry SML, Ritchie RO (1993) Metal Mater Trans 24A:585
13. Miura S, Shimamura H, Fujinaka J, Mohri TJ (2004) Intermetallics 12:771
14. Alman DE (2005) Intermetallics 13:572
15. Peng LM, Li Z, Li H, Wang JH, Gong M (2006) J Alloys Comp 414:100
16. ASTM Standard E399-83 (1990) Annual book of ASTM standards, Section 3, American Society for Testing and Materials, Philadelphia, PA, p 500
17. Oehring M, Klassen T, Bormann R (1993) J Mater Res 8:2819
18. Godfrey A, Hu D, Loretto MH (1997) Mater Sci Eng A A239–240:559
19. Banumathy S, Ghosal P, Singh AK (2005) J Alloys Comp 394:181
20. Thomas M, Raviart JL, Popoff F (2005) Intermetallics 13:944
21. Oehring M, Bormann R (1990) J Physique 51 (Coll. C4) 169
22. Buta F (2003) PhD Dissertation, The Ohio State University, USA
23. Buta F, Sumption MD, Collings EW (2003) IEEE Trans Appl Supercon 13:3462
24. Chen GL, Zhang WJ, Liu ZC, Li SJ (1999) In Kim Y-W, Dimiduk DM, Loretto MH (eds) Gamma titanium aluminides. Warrendale, PA, p 371